OPEN

Meaning of Intracranial Pressure-to-Blood Pressure Fisher-Transformed Pearson Correlation–Derived Optimal Cerebral Perfusion Pressure: Testing Empiric Utility in a Mechanistic Model

Alireza Akhondi-Asl, PhD[1]; Frederick W. Vonberg, MBBS[1]; Cheuk C. Au, MBBS[1]; Robert C. Tasker, MD, FRCP[1,2]

Objectives: Time-averaged intracranial pressure-to-blood pressure Fisher-transformed Pearson correlation (PR_x) is used to assess cerebral autoregulation and derive optimal cerebral perfusion pressure. Empirically, impaired cerebral autoregulation is considered present when PR_x is positive; greater difference between time series median cerebral perfusion pressure and optimal cerebral perfusion pressure (Δ_{CPP}) is associated with worse outcomes. Our aims are to better understand: 1) the potential strategies for targeting optimal cerebral perfusion pressure; 2) the relationship between cerebral autoregulation and PR_x; and 3) the determinants of greater Δ_{CPP}.

Design: Mechanistic simulation using a lumped compartmental model of blood pressure, intracranial pressure, cerebral autoregulation, cerebral blood volume, $Paco_2$, and cerebral blood flow.

Setting: University critical care integrative modeling and precision physiology research group.

Subjects: None, in silico studies.

Interventions: Simulations in blood pressure, intracranial pressure, $Paco_2$, and impairment of cerebral autoregulation, with examination of "output" cerebral perfusion pressure versus PR_x-plots, optimal cerebral perfusion pressure, and Δ_{CPP}.

Measurements and Main Results: In regard to targeting optimal cerebral perfusion pressure, a shift in mean blood pressure or mean intracranial pressure with no change in mean blood pressure, with intact cerebral autoregulation, impacts optimal cerebral perfusion pressure. Second, a positive PR_x occurs even with intact cerebral autoregulation. In relation to Δ_{CPP}, for a given input blood pressure profile, with constant intracranial pressure, altering the degree of impairment in cerebral autoregulation or the level of $Paco_2$ maintains differences to within ±5 mm Hg. Change in intracranial pressure due to either an intermittently prolonged pattern of raised intracranial pressure or terminal escalation shows Δ_{CPP} greater than 10 mm Hg and less than −10 mm Hg, respectively.

Conclusions: These mechanistic simulations provide insight into the empiric basis of optimal cerebral perfusion pressure and the significance of PR_x and Δ_{CPP}. PR_x and optimal cerebral perfusion pressure deviations do not directly reflect changes in cerebral autoregulation but are, in general, related to the presence of complex states involving well-described clinical progressions with raised intracranial pressure. (*Crit Care Med* 2018; 46:e1160–e1166)

Key Words: blood pressure; cerebral autoregulation; cerebral blood flow; cerebral hemodynamics; intracranial pressure; mathematical modeling

[1]Department of Anesthesiology, Critical Care and Pain Medicine, Boston Children's Hospital and Harvard Medical School, Boston, MA.

[2]Department of Neurology, Boston Children's Hospital and Harvard Medical School, Boston, MA.

Supplemental digital content is available for this article. Direct URL citations appear in the printed text and are provided in the HTML and PDF versions of this article on the journal's website (http://journals.lww.com/ccmjournal).

Supported, in part, by a Trailblazer award from the Department of Anesthesiology, Critical Care and Pain Medicine, at Boston Children's Hospital, Boston, MA.

Dr. Akhondi-Asl received other support from a Trailblazer Award. Dr. Tasker received funding from a "Trailblazer Award" from the Department of Anesthesiology, Perioperative and Pain Medicine, at Boston Children's Hospital, Boston, MA. The remaining authors have disclosed that they do not have any potential conflicts of interest.

For information regarding this article, E-mail: Robert.tasker@childrens.harvard.edu

DOI: 10.1097/CCM.0000000000003434

A key concern in the management of patients with severe traumatic brain injury (TBI) is whether cerebral autoregulation (CA) is intact and able to minimize alterations in cerebral blood flow (CBF) due to changes in cerebral perfusion (1–3). Because there are a number of processes underlying CA and CBF control, we have two main clinical challenges to consider: variance in the upper and lower limits of CA, and not knowing patient-specific optimal levels in

intrinsic physiologic factors such as $Paco_2$, blood pressure (BP), and intracranial pressure (ICP) (4–6).

These are two general approaches studying indirectly whole brain circulation pathophysiology (6). First, an empirical approach using observational and epidemiologic evidence to establish statistical relationships and correlations between inputs and outputs. This approach is best exemplified by studies in severe TBI using ICP to BP Fisher-transformed Pearson correlation ("PR_x") (i.e., 5–7 min of time-averaged ICP and BP data to calculate mean Fisher-transformed Pearson correlation) to derive, by statistical analyses, the cerebral perfusion pressure (CPP, the difference between mean BP and mean ICP) optimal for an individual (i.e., optimal CPP [CPP_{Opt}]). Briefly, by inference, because positive PR_x is considered representative of disturbed CA and negative PR_x is reflective of intact CA (7), the CPP_{Opt} is defined as the CPP at which PR_x is at its minimum (7–10). In severe TBI, the difference between contemporaneous time series median CPP (CPP_{Med}) and CPP_{Opt} (i.e., difference between time series CPP_{Med} and CPP_{Opt} [Δ_{CPP}]) 0–5 mm Hg is associated with favorable outcome, whereas Δ_{CPP} −10 to −15 mm Hg occurs only in those with unfavorable outcome (8). Such empiric associations can lead to new hypotheses and, possibly, pragmatic trials. However, these observations cannot provide better understanding of pathophysiology or even the determinants of CPP_{Opt}. Second, we have a mechanistic approach to indirect assessment of global cerebrovascular behavior using electrical analog models of CA control pathways, feedback loops, and arterial network structure (2, 3, 7, 11–20). Here, in silico evidence is rationalized according to the fluid dynamics or electronics of inputs and outputs. In 1988, Ursino (11, 12) proposed the first "lumped compartmental model" of cerebral circulation physiology that included CA. Since then, the modeling mechanistic approach has been used to better understand patient data from, for example, transcranial Doppler studies of middle cerebral artery flow velocity (6, 21, 22). To date, such models have not been used to provide mechanistic insight into the questions of "What does PR_x-derived CPP_{Opt} mean?" and "What is the effect of manipulating BP, ICP and $Paco_2$?"

In this report, we use the lumped compartmental model of brain circulation physiology and CA, with its system operating CPP, to assess PR_x and calculated CPP_{Opt}. Our aims are to simulate the physiology in severe TBI and better understand: 1) the potential strategies for targeting CPP_{Opt}; 2) the relationship between CA and PR_x; and 3) the determinants of Δ_{CPP}.

MATERIALS AND METHODS

This experimental in silico study did not require Local Ethics Committee approval.

Lumped Compartmental Model of CA

We have implemented the model by Ursino et al (2), Ursino and Giannessi (3), Ursino (11, 12), and Ursino and Lodi (13, 14) to first test potential strategies for targeting CPP_{Opt}. **Figure 1** shows the electrical analog of our model with its four compartments that account for interactions among BP, ICP, CA, cerebral blood volume, $Paco_2$, and CBF. **Supplemental Digital Content 1** (http://links.lww.com/CCM/D992) provides more information about the model and the transient 6-hour change in BP profile (with 50 Hz sampling rate) used in the simulations (11, 14, 23). At baseline, the model operates with BP, CPP, CBF, and ICP at 100 mm Hg, 90.5 mm Hg, 12.5 mL/s (750 mL/min), and 10 mm Hg, respectively.

PR_x and Estimation of CPP_{Opt}

We have simulated changes in BP, $Paco_2$, CA state, and ICP (by fluid injection into the cerebrospinal fluid [CSF] space). CPP is calculated from BP and ICP signals. CPP_{Med} is the CPP_{Med} for the whole simulation.

To compute PR_x, we average BP and ICP over 10 seconds, and then use 40 consecutive time-averaged samples. Individual correlations are collated throughout the simulation. Mean CPP during each time series correlation calculation is then associated with the individual PR_x. Then, the range in these mean CPP values is divided into 5 mm Hg width "bins," and the mean PR_x corresponding to each bin is plotted—hereafter called the "PR_x-plot." We use these data in another exploratory plot to calculate the minimum of the curve that defines CPP_{Opt} (4, 7, 8, 24). The Δ_{CPP} is also evaluated as a difference category ($\Delta_{Category}$) according to previously used ranges (9).

RESULTS

Figure 1 shows the steady-state characteristics of the electrical analog model under conditions of $Paco_2$ variation and CA gain. There is the expected dependence of CBF on CPP: for any given value in CPP, an increase in $Paco_2$ causes the expected increase in CBF, whereas a decrease in $Paco_2$ leads to the expected decrease in CBF (**Fig. 1*B***). **Figure 1*C*** shows that when CA is impaired, there is more significant alteration in CBF with variation in CPP.

Potential Influencers of CPP_{Opt}

Change in BP. We tested different BP profiles using fully intact CA and constant ICP and $Paco_2$, 10 and 40 mm Hg, respectively. An example of the full graphical process for each "input" BP to "output" PR_x-plot is shown in **Figure S1** (Supplemental Digital Content 2, http://links.lww.com/CCM/E35). **Figure S2** (Supplemental Digital Content 2, http://links.lww.com/CCM/E35) shows that degree and pattern of change in BP impact the PR_x-plot and derivation of CPP_{Opt}.

Figure 2 shows the effect of shifting by a fixed amount one of the BP profiles from **Figure S2*E*** (Supplemental Digital Content 2, http://links.lww.com/CCM/E35—see *bold black line* originating at 80 mm Hg), thereby maintaining the same BP profile but with different median BP (BP_{Med}) during the whole simulation (**Table S1**, Supplemental Digital Content 3, http://links.lww.com/CCM/E36). A shift in BP_{Med} (**Fig. 2*A***) has an impact on the position of the minimum in the PR_x-plots (**Fig. 2*B***) and CPP_{Opt} (Table S1, Supplemental Digital Content 3, http://links.lww.com/CCM/E36). A downward shift in BP profile by 10 mm Hg, from the line originating at 80 mm Hg (Fig. 2*A*, *black line*) to the line originating at 70 mm Hg, leads to a similar 10 mm Hg downward

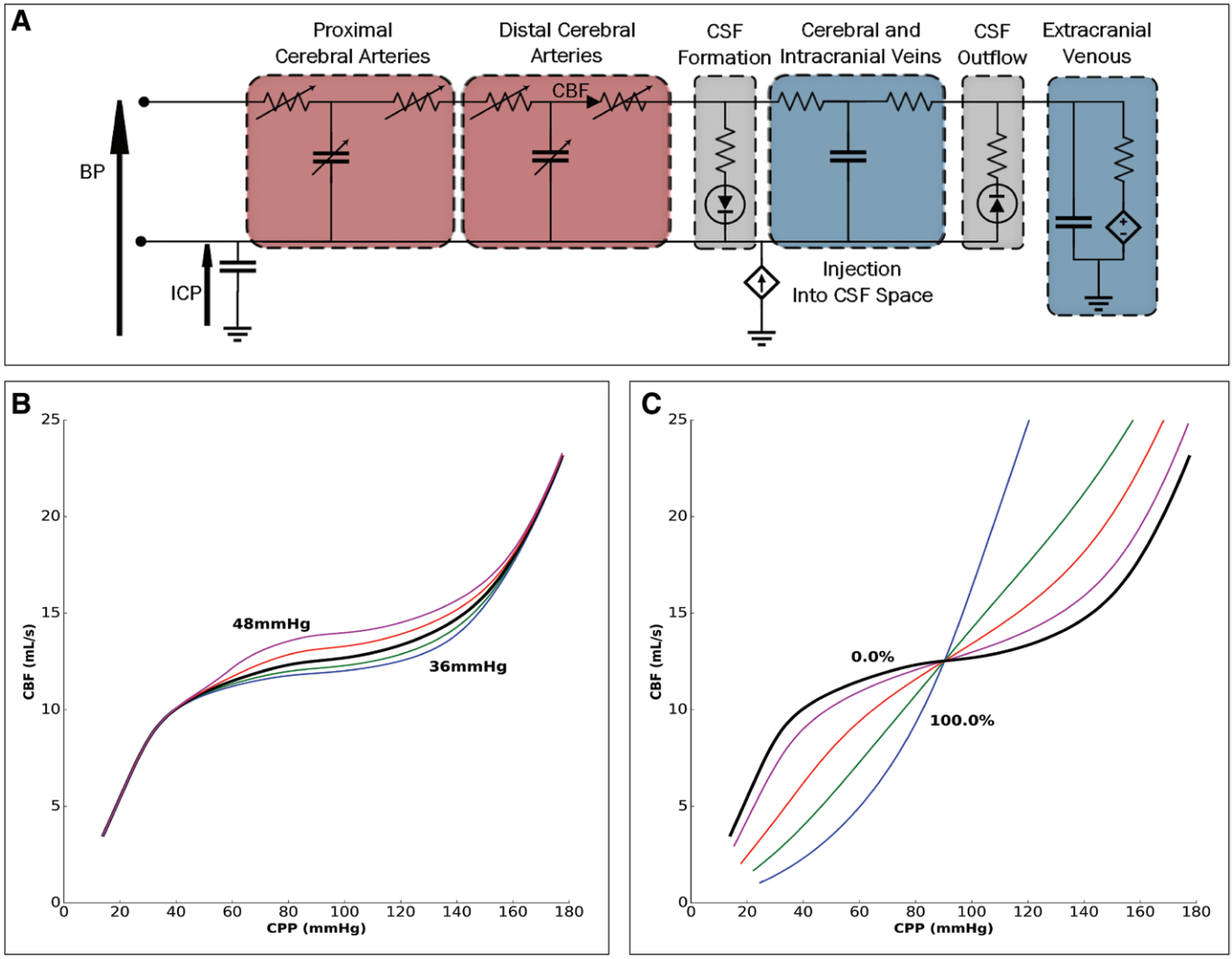

Figure 1. The electrical circuit equivalent of the lumped compartment model and some baseline physiologic operating characteristics. **A**, The model includes different segments: proximal and distal cerebral arteries, cerebral and intracranial veins, extracranial venous, and cerebrospinal fluid (CSF) formation and outflow. **B**, The dependence of cerebral blood flow (CBF) on cerebral perfusion pressure (CPP) under steady-state conditions at various $Paco_2$ values (36, 38, 40, 42, and 44 mm Hg). Increasing $Paco_2$ increases CBF at any given CPP. **C**, The dependence of CBF on CPP when cerebral autoregulation (CA) gain varies. CPP variation leads to more alteration in CBF as CA impairment increases (0%, 25%, 50%, 75%, and 100%). BP = blood pressure, ICP = intracranial pressure.

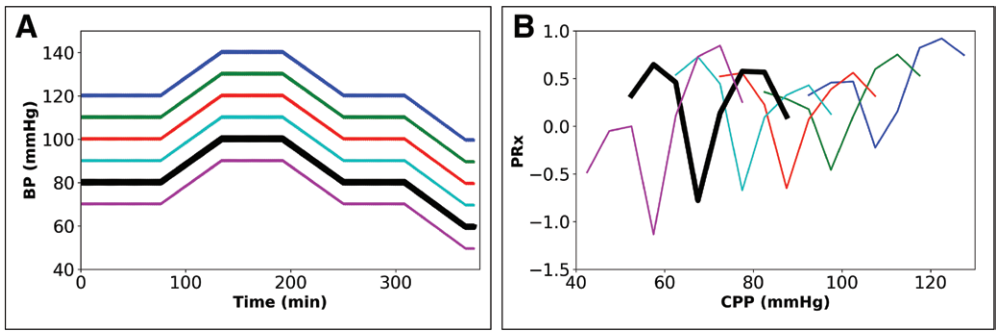

Figure 2. Impact of shifting the 6-hr mean blood pressure (BP) profile on intracranial pressure-to-BP Fisher-transformed Pearson correlation (PR_x) when cerebral autoregulation is intact. Paired graphs with input BP profiles (A) and output cerebral perfusion pressure (CPP) PR_x-plots before final curve fitting (for details and text, see Fig. S2, Supplemental Digital Content 2, http://links.lww.com/CCM/E35). **A**, BP profile shifted either up or down by fixed amount, giving six inputs differing in mean BP. **B**, Output PR_x-plots for profiles in **A**, showing that difference in mean BP, but fixed pattern, results in shift in the minima in the plots (for results of final mathematical transformation to calculate optimal CPP [see text], see Table S1, Supplemental Digital Content 3, http://links.lww.com/CCM/E36).

shift in CPP_{Med} (from 71 to 61 mm Hg) and similar downward shift in CPP_{Opt} (from 68 to 56 mm Hg) (Table S1, Supplemental Digital Content 3, http://links.lww.com/CCM/E36). On inspecting these data with the same BP profile, BP_{Med} or CPP_{Med} (if ICP is at a constant level) determines the position of CPP_{Opt}.

Change in $Paco_2$. The impact of change in $Paco_2$ on CPP_{Opt} is minimal (**Fig. S3**, Supplemental Digital Content 2, http://links.lww.com/CCM/E35; and Table S1,

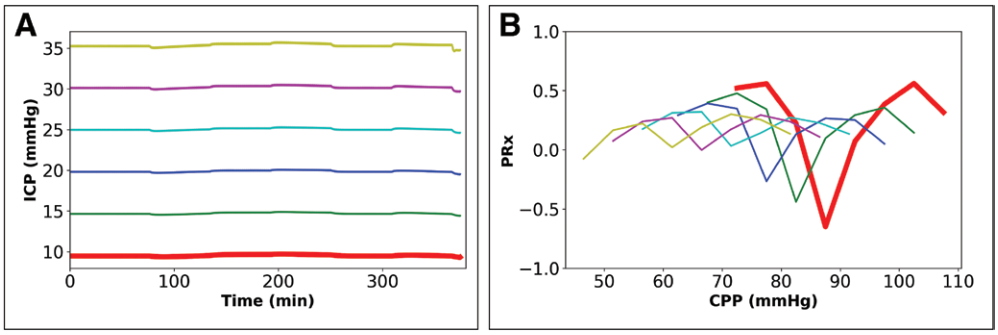

Figure 3. Impact of fixed change in mean intracranial pressure (ICP) profile over 6 hr when cerebral autoregulation is intact and $Paco_2$ is 40 mm Hg. Paired graphs with input ICP profiles (A) and output cerebral perfusion pressure (CPP) ICP-to-blood pressure (BP) Fisher-transformed Pearson's correlation (PR_x) plots before final curve fitting (the BP profile is the same in all simulations). **A**, The effect of injection of fluid into the cerebrospinal fluid space at six different rates (0.0–0.05 mL/s) to raise mean ICP to six constant levels (10, 15, 20, 25, 30, and 35 mm Hg). **B**, Output PR_x-plots for profiles in (**A**) showing shift similar to that seen with fixed alteration in BP (Fig. 2*B* for comparison; for results of final mathematical transformation to calculate optimal CPP, see Table S1, Supplemental Digital Content 3, http://links.lww.com/CCM/E36).

Supplemental Digital Content 3, http://links.lww.com/CCM/E36). Alterations in $Paco_2$ (32–48 mm Hg) lead to small changes in ICP and little impact on the position of the minimum in the PR_x-plots. The increase in CPP_{Opt} with increase in $Paco_2$ from 32 to 48 mm Hg was 5 mm Hg (87–92 mm Hg).

Change in ICP. The effects of changes in ICP profile—when CA is intact and 40 mm Hg $Paco_2$—on the PR_x-plot show increasing shift with constantly increased ICP. When using the BP profile from Figure 2*A* (see *red line* originating at 100 mm Hg) with six constant levels in ICP, the output PR_x-plots are shown (**Fig. 3**). For comparison, **Figure S4** (Supplemental Digital Content 2, http://links.lww.com/CCM/E35), using the BP profile in **Fig. S2*C*** (Supplemental Digital Content 2, http://links.lww.com/CCM/E35), illustrates the output PR_x-plots with the same constant shift in ICP). Figure 3 and Table S1 (Supplemental Digital Content 3, http://links.lww.com/CCM/E36) show that a constant shift of 10 mm Hg (from 20 to 30 mm Hg) results in a downward shift in CPP_{Med} by 9 mm Hg (from 81 to 70 mm Hg). CPP_{Opt} also decreases by 9 mm Hg (from 79 to 70 mm Hg). Therefore, similar to the findings in Figure 2, *A* and *B*, the position of CPP_{Opt} is determined by constant rise in ICP level or constant change in CPP with a constant BP profile.

Figures 4 and **5** use the same BP profile to Figure S2*C* (see also Fig. S4, Supplemental Digital Content 2, http://links.lww.com/CCM/E35). (Table S1 [Supplemental Digital Content 3, http://links.lww.com/CCM/E36] shows for comparison the findings when using the ICP profiles in Fig. 3*A* with the BP profile from Fig. S2*C* [Supplemental Digital Content 2, http://links.lww.com/CCM/E35].) Figure 4 shows the effect of a series of peaks in ICP. (Of note, **Fig. S5*E*** [Supplemental Digital Content 2, http://links.lww.com/CCM/E35] shows that during such wave-like changes, PR_x goes from a negative value to a positive value, and back to a negative value in the course of each wave in ICP.) An upward shift in peak ICP by 10 mm Hg (20–30 mm Hg) results in minimal downward shift in CPP_{Med} by approximately 2 mm Hg (from 86 to 84 mm Hg), but CPP_{Opt} shows an upward shift by approximately 10 mm Hg (from 63 to 73 mm Hg).

Figure 5 shows the effect of an escalation in ICP profile, with the same BP profile used in Figure 4. In this instance, an upward shift in the final peak in ICP by 10 mm Hg (20–30 mm Hg at peak) results in downward shift in CPP_{Med} by 10 mm Hg (from 78 to 68 mm Hg), but CPP_{Opt} exhibits a smaller downward shift (≈4 mm Hg, from 85 to 81 mm Hg) (Table S1, Supplemental Digital Content 3, http://links.lww.com/CCM/E36).

CA and PR_x

At baseline state (40 mm Hg $Paco_2$ and 10 mm Hg ICP with consistent BP profile), change in CA gain—an indicator of impairment of feedback systems—has minimal consequence on the position of the minimum in the PR_x-plots (Table S1, Supplemental Digital Content 3, http://links.lww.com/CCM/E36). The increase in CPP_{Opt} with increasingly impaired CA from 0% to 50% was small (≈2 mm Hg, from 89 to 91 mm Hg). However, mean PR_x at CPP_{Opt} changes –0.14 to 0.25, to 0.80 with increase in CA impairment from 0% to 25%, to 50%, respectively.

On inspection of Table S1 (Supplemental Digital Content 3, http://links.lww.com/CCM/E36), it is also evident that in simulations with fully intact CA, it is still possible to obtain a positive mean PR_x at so-called CPP_{Opt}; that is, a positive coefficient is not necessarily

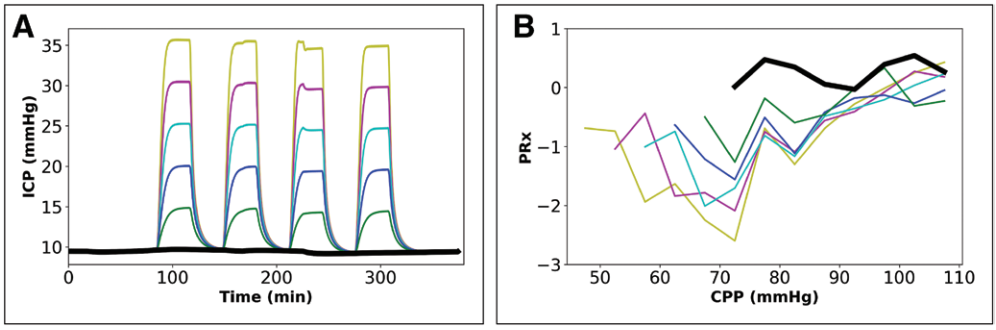

Figure 4. Impact of serial peaks in intracranial pressure (ICP) over 6 hr, when cerebral autoregulation is intact and $Paco_2$ is 40 mm Hg. Paired graphs with input ICP profiles (**A**) and output cerebral perfusion pressure (CPP) ICP-to-blood pressure (BP) Fisher-transformed Pearson correlation (PR_x) plots before final curve fitting (the BP profile is the same in all simulations). **A**, Four serial peaks in ICP with five different peak levels (color-coding similar to Fig. 3, see text for details). **B**, Output PR_x-plots for profiles in **A**, (for results of final mathematical transformation to calculate optimal CPP, see Table S1, Supplemental Digital Content 3, http://links.lww.com/CCM/E36).

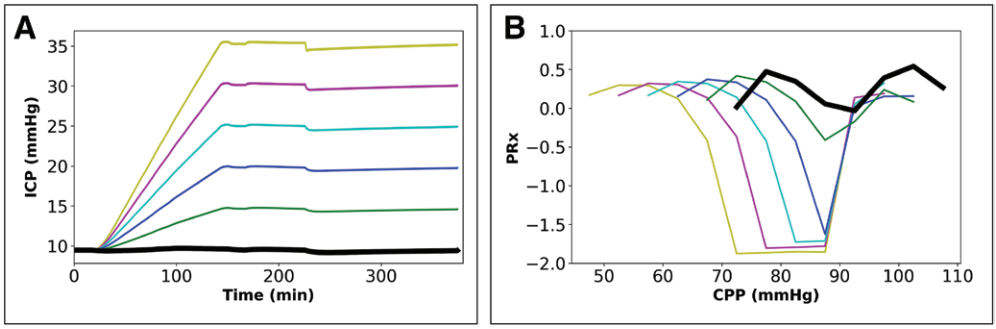

Figure 5. Impact of escalation in intracranial pressure (ICP) profile over 6 hr to a terminal plateau when cerebral autoregulation is intact and $Paco_2$ is 40 mm Hg. Paired graphs with input ICP profiles (**A**) and output cerebral perfusion pressure (CPP) ICP-to-blood pressure (BP) Fisher-transformed Pearson correlation (PR_x) plots before final curve fitting (the BP profile is the same in all simulations). **A**, Five patterns of escalation in ICP (color-coding similar to Fig. 3, see text for details). **B**, Output PR_x-plots for profiles in **A**, showing shift in curves (for results of final mathematical transformation to calculate optimal CPP, see Table S1, Supplemental Digital Content 3, http://links.lww.com/CCM/E36).

an indicator of impaired CA. (**Fig. S6** [Supplemental Digital Content 2, http://links.lww.com/CCM/E35] summarizes the findings of a full analysis with 756 separate simulations, which comes to the same conclusion as Table S1, Supplemental Digital Content 3, http://links.lww.com/CCM/E36.)

The Determinants of Δ_{CPP}

A fixed change in BP (Fig. 2*A*) or a constant rise in ICP (**Fig. 3*A***), using the same BP profile, resulted in Δ_{CPP} values in the $\Delta_{Category}$ 0–5 mm Hg (Table S1, Supplemental Digital Content 3, http://links.lww.com/CCM/E36). We could only simulate a state with $\Delta_{Category}$ 5–10 mm Hg when selecting a lower BP profile (with constant ICP 10 mm Hg), and CPP_{Med} approximately 61 mm Hg. We could simulate Δ_{CPP} –19.9 mm Hg if we used a different BP profile (Fig. S2*C*, Supplemental Digital Content 2, http://links.lww.com/CCM/E35) and constantly raised ICP of 25 mm Hg.

In the simulations with serial peaks in ICP (20–35 mm Hg; Fig. 4), the $\Delta_{Category}$ was consistently greater than 10 mm Hg (Table S1, Supplemental Digital Content 3, http://links.lww.com/CCM/E36). Last, an escalating rise in ICP (Fig. 5) with peak 15–25 mm Hg resulted in $\Delta_{Category}$ –10 to –5 mm Hg. An escalating ICP peak 30–35 mm Hg resulted in $\Delta_{Category}$ less than –10 mm Hg (Table S1, Supplemental Digital Content 3, http://links.lww.com/CCM/E36).

DISCUSSION

PR_x-derived CPP_{Opt}, with calculation of Δ_{CPP} and $\Delta_{Category}$, are statistical constructs and have proven value in patient risk stratification and in epidemiologic association with poor outcome (4, 7–9, 23–26). However, CPP is not physiologically controlled in homeostasis; there is no sensor, error signal, set point, or optimum within the operating range between the upper and lower limits of CA. Hence, CPP_{Opt}-guided management may be a testable pragmatic therapeutic approach, but, intrinsically, empiricism has limitations to understanding mechanistic functions (27). How could a mechanistic model of cerebrovascular pathophysiology improve on an empirical approach that is already able to predict outcome during real-time monitoring of BP and ICP in severe TBI? In this report, we describe three insights. First, in regard to targeting CPP_{Opt}, a shift in BP_{Mean} or mean ICP, with intact CA, impacts CPP_{Opt}. Second, a positive PR_x at CPP_{Opt}, which should signify impaired CA, in the lumped model also occurs with intact CA. Last, in relation to Δ_{CPP}, the compartmental model confirms that greater deviation from zero is associated with more severe 6-hour profiles in ICP.

We should first note potential limitations in our simulations. Our model simplifies a complex system. We could add more feedback systems, but have settled on the balance between complexity and the ability to model a system, which is an approach now commonly used in so-called "personalized, model-based critical care medicine" (28). Other limitations of the model are that CBF is derived without accounting for changes in cerebral metabolism, the effects of medications or CSF diversion on cerebrovascular dynamics, and the consequence of surgical interventions (e.g., craniotomy, hematoma evacuation). Neither does the model account for brain heterogeneity in CA and microvascular nonnutritive phenomena such as shunt flow (29). That said, there are four advantages of our in silico testing: 1) "ground truth" CA is known and model parameters can be set to desired values; 2) changes in BP and ICP can be controlled and examined; 3) confounding factors can be controlled or eliminated; and 4) measurement errors can be removed as noise level can be controlled.

Potential Strategies for Targeting CPP_{Opt}

Our first finding about strategies in targeting CPP_{Opt} when CA is intact found that shift in either BP or ICP has an impact on CPP_{Opt}. CPP_{Opt} is also sensitive to the low-frequency characteristics of the BP and ICP profiles. Because CPP is a derived variable and mathematically coupled to both BP and ICP, we show in a separate mathematical analysis that CPP_{Opt} can change just by changing the input BP or ICP profiles, which confirms the findings in our simulations (**Supplemental Digital Content 4**, http://links.lww.com/CCM/E37). The equations also show that even when PR_x does not change substantially, there can be significant change in CPP_{Opt}. These features may explain why PR_x-derived CPP_{Opt} has applications in pediatric severe TBI even though children have lower BP (10, 30). Returning to adult severe TBI, a recent analysis of CPP_{Opt} in 104 patients managed in two European centers found heterogeneity in CPP_{Opt} between the centers, which was attributed to different management protocols, especially different CPP targets, and different demographic factors like age-related BP_{Mean} (31). Our report provides in silico and mathematical underpinnings for these

expected observations and an explanation as to how these factors should be considered in practice.

CA and PR_x

In theory, a positive PR_x should be associated with impaired CA, whereas negative values should reflect intact CA. In our simulations, we found that even when CA is fully intact, it is possible to obtain a positive mean PR_x at the value of CPP_{Opt}, which is at odds with the pressure reactivity concept. In the mathematical analysis (Supplemental Digital Content 4, http://links.lww.com/CCM/E37), the equations confirm that impairment of CA will have an impact on PR_x, but no major difference in Δ_{CPP}, which in our simulations remained within ±5 mm Hg (see below). That said, under controlled conditions, in which impairment in CA is known to be present, more positive PR_x does reflect more severe impairment. However, when using only ICP, BP, and CPP data, we cannot always know whether CA is impaired or not. Hence, taken in isolation, monitoring PR_x is not providing added information about CA.

$\Delta_{Category}$ and Outcome

Several clinical studies have used the PRx-based estimate of CPP_{Opt} (4, 7–10, 24–26) with some adult patient cohorts demonstrating an association between outcome after severe TBI and $\Delta_{Category}$ (9, 25). In a case series of 299 adults with severe TBI, Aries et al (8) found the following: when their summary of $\Delta_{Category}$ for the whole period of ICP monitoring (using a moving window of 4 hr over and average of 4 d of data) was less than –10 mm Hg, all patients died; when their summary $\Delta_{Category}$ was greater than 10 mm Hg, approximately 30% survived with favorable outcome, approximately 60% survived with severe disability, and the remainder died. Our simulations add to the face validity of these associations and also provide further insight. They show that during constant decrease in BP or nonextreme constant increase in ICP, shift in CPP_{Opt} is similar to shift in CPP_{Med}, and so the Δ_{CPP} remains within ±5 mm Hg. The mathematical handling (Supplemental Digital Content 4, http://links.lww.com/CCM/E37) also indicates that even when CA impairment has an impact on PR_x, there may not be a major change in Δ_{CPP}, which in our simulations also remained within ±5 mm Hg. In order to generate a $\Delta_{Category}$ more typical of those associated with poor outcomes in the clinical literature (8, 25), our simulations needed to incorporate a major abnormality in ICP 6-hour profile. A constant ICP at 25 mm Hg or escalation in ICP without remission to greater than 30 mm Hg gave $\Delta_{Category}$ less than –10 mm Hg. A series of peaks in ICP up to 20–35 mm Hg resulted in $\Delta_{Category}$ greater than 10 mm Hg.

CONCLUSIONS

Taken together, our simulations provide mechanistic insight into the interpretation of PR_x, CPP_{Opt}, and $\Delta_{Category}$. These empirically derived variables do provide a numerical summary of complex states involving well-described clinical progression and deterioration with raised ICP (32). This feature has epidemiologic importance, and we also wonder whether these composite indices may serve to provide a threshold for shift in treatment paradigm when managing cases with severe TBI—such as moving from medical to surgical interventions. Last, as illustrated by this report, the value of empirical and model-based mechanistic approaches in critical care medicine should be considered as complementary and potentially synergistic (27).

REFERENCES

1. Lassen NA: Cerebral blood flow and oxygen consumption in man. *Physiol Rev* 1959; 39:183–238
2. Ursino M, Di Giammarco P, Belardinelli E: A mathematical model of cerebral blood flow chemical regulation–Part I: Diffusion processes. *IEEE Trans Biomed Eng* 1989; 36:183–191
3. Ursino M, Giannessi M: A model of cerebrovascular reactivity including the circle of Willis and cortical anastomoses. *Ann Biomed Eng* 2010; 38:955–974
4. Czosnyka M, Smielewski P, Kirkpatrick P, et al: Continuous assessment of the cerebral vasomotor reactivity in head injury. *Neurosurgery* 1997; 41:11–17
5. Panerai RB, Chacon M, Pereira R, et al: Neural network modelling of dynamic cerebral autoregulation: Assessment and comparison with established methods. *Med Eng Phys* 2004; 26:43–52
6. Payne S: Cerebral Autoregulation: Control of Blood Flow in the Brain. Berlin, Germany, Springer, 2016
7. Steiner LA, Czosnyka M, Piechnik SK, et al: Continuous monitoring of cerebrovascular pressure reactivity allows determination of optimal cerebral perfusion pressure in patients with traumatic brain injury. *Crit Care Med* 2002; 30:733–738
8. Aries MJ, Czosnyka M, Budohoski KP, et al: Continuous determination of optimal cerebral perfusion pressure in traumatic brain injury. *Crit Care Med* 2012; 40:2456–2463
9. Lazaridis C, Smielewski P, Steiner LA, et al: Optimal cerebral perfusion pressure: Are we ready for it? *Neurol Res* 2013; 35: 138–148
10. Lewis PM, Czosnyka M, Carter BG, et al: Cerebrovascular pressure reactivity in children with traumatic brain injury. *Pediatr Crit Care Med* 2015; 16:739–749
11. Ursino M: A mathematical study of human intracranial hydrodynamics. Part 1–The cerebrospinal fluid pulse pressure. *Ann Biomed Eng* 1988; 16:379–401
12. Ursino M: A mathematical study of human intracranial hydrodynamics part 2–Simulation of clinical tests. *Ann Biomed Eng* 1988; 16: 403–416
13. Ursino M, Lodi CA: A simple mathematical model of the interaction between intracranial pressure and cerebral hemodynamics. *J Appl Physiol (1985)* 1997; 82:1256–1269
14. Ursino M, Lodi CA: Interaction among autoregulation, CO_2 reactivity, and intracranial pressure: A mathematical model. *Am J Physiol* 1998; 274:H1715–H1728
15. Piechnik S, Czosnyka M, Smielewski P, et al: Indices for decreased cerebral blood flow control–A modelling study. *Acta Neurochir Suppl* 1998; 71:269–271
16. Banaji M, Tachtsidis I, Delpy D, et al: A physiological model of cerebral blood flow control. *Math Biosci* 2005; 194:125–173
17. Payne S: A model of the interaction between autoregulation and neural activation in the brain. *Math Biosci* 2006; 204:260–281
18. Spronck B, Martens EG, Gommer ED, et al: A lumped parameter model of cerebral blood flow control combining cerebral autoregulation and neurovascular coupling. *Am J Physiol Heart Circ Physiol* 2012; 303:H1143–H1153
19. Hu X, Nenov V, Bergsneider M, et al: Estimation of hidden state variables of the intracranial system using constrained nonlinear Kalman filters. *IEEE Trans Biomed Eng* 2007; 54:597–610
20. Silvani A, Magosso E, Bastianini S, et al: Mathematical modeling of cardiovascular coupling: Central autonomic commands and baroreflex control. *Auton Neurosci* 2011; 162:66–71

21. Ursino M, Giulioni M: Quantitative assessment of cerebral autoregulation from transcranial Doppler pulsatility: A computer simulation study. *Med Eng Phys* 2003; 25:655–666
22. Aoi MC, Kelley C, Novak V, et al: Optimization of a mathematical model of cerebral autoregulation using patient data. *IFAC Proc Vol* 2009; 42:181–186
23. Alastruey J, Parker K, Peiró J, et al: Lumped parameter outflow models for 1-D blood flow simulations: Effect on pulse waves and parameter estimation. *Commun Comput Phys* 2008; 4:317–336
24. Bijlenga P, Czosnyka M, Budohoski KP, et al: "Optimal cerebral perfusion pressure" in poor grade patients after subarachnoid hemorrhage. *Neurocrit Care* 2010; 13:17–23
25. Zweifel C, Lavinio A, Steiner LA, et al: Continuous monitoring of cerebrovascular pressure reactivity in patients with head injury. *Neurosurg Focus* 2008; 25:E2
26. Petkus V, Krakauskaitė S, Preikšaitis A, et al: Association between the outcome of traumatic brain injury patients and cerebrovascular autoregulation, cerebral perfusion pressure, age, and injury grades. *Medicina (Kaunas)* 2016; 52:46–53
27. Baker RE, Pena J-M, Jayamohan J, et al: Mechanistic models versus machine learning, a fight worth fighting for the biological community? *Biol Lett* 2018; 14:20170660
28. Chase JG, Preiser JC, Dickson JL, et al: Next-generation, personalised, model-based critical care medicine: A state-of-the art review of in silico virtual patient models, methods, and cohorts, and how to validation them. *Biomed Eng Online* 2018; 17:24
29. Dai X, Bragina O, Zhang T, et al: High intracranial pressure induced injury in the healthy rat brain. *Crit Care Med* 2016; 44: e633–e638
30. Young AM, Donnelly J, Czosnyka M, et al: Continuous multimodality monitoring in children after traumatic brain injury-preliminary experience. *PLoS One* 2016; 11:e0148817
31. Howells T, Smielewski P, Donnelly J, et al: Optimal cerebral perfusion pressure in centers with different treatment protocols. *Crit Care Med* 2018; 46:e235–e241
32. Lundberg N: Continuous recording and control of ventricular fluid pressure in neurosurgical practice. *Acta Psychiatr Scand Suppl* 1960; 36:1–193